

e28 Atlas of Clinical Imaging of the Vasculitic Diseases

Carol A. Langford, Anthony S. Fauci

Diagnostic imaging represents a critical assessment tool in patients who are known or suspected to have a systemic vasculitic disease. Imaging contributes unique information about the patient that, when taken together with the history, physical examination, and laboratory determinations, can guide the differential diagnosis and the subsequent assessment or treatment plan. A diverse range of imaging techniques are utilized in the assessment of vasculitis including plain radiography, ultrasonography, CT, MRI, positron emission tomography, and catheter-directed dye arteriography. These procedures have specific utilities that can allow differing perspectives on the spectrum and severity of vasculitis.

For vasculitic diseases that involve the large- or medium-sized blood vessels, arteriography provides information regarding blood vessel stenoses or aneurysms that can support the diagnosis. Catheter-directed dye arteriography offers the most precise information regard-

ing the vessel lumen but carries risks related to dye exposure and the invasive nature of the procedure. Advancements in MR and CT arteriography have brought about noninvasive options to view the lumen and vessel wall, thus enhancing the ability to perform serial studies for patient monitoring.

Although vasculitis involving the small blood vessels cannot be directly visualized, diagnostic imaging plays an essential role in detecting tissue injury that occurs as result of blood vessel and tissue inflammation. In Wegener's granulomatosis, 80% of patients may have pulmonary involvement during their disease course. Chest imaging should be obtained whenever active disease is suspected, as up to one-third of patients with radiographic abnormalities are asymptomatic. Pulmonary imaging is also important to detect complications of vasculitis therapy such as opportunistic pneumonias as well as medication-related pneumonitis.

The images provided in this Atlas highlight the utility of diagnostic imaging in the vasculitic diseases and the improvements in the care of vasculitis patients that have resulted from radiologic innovations. With the rapid growth in precision and techniques, the role of diagnostic imaging will continue to enhance the ability of physicians to detect, monitor, and diagnose vasculitis noninvasively.

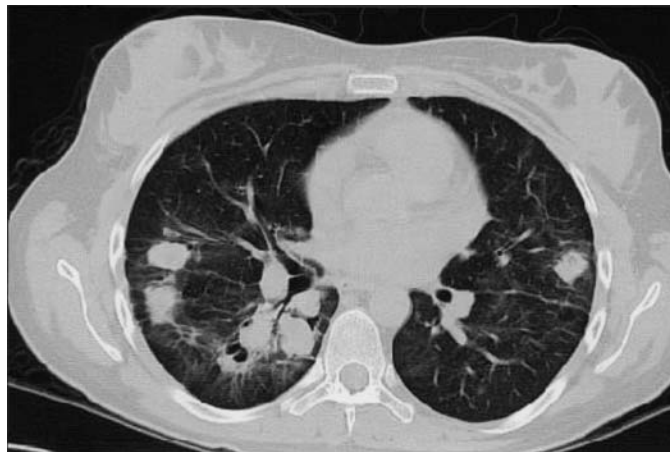


FIGURE e28-1 Bilateral nodular infiltrates seen on computed tomography of the chest in a 40-year-old woman with Wegener's granulomatosis.

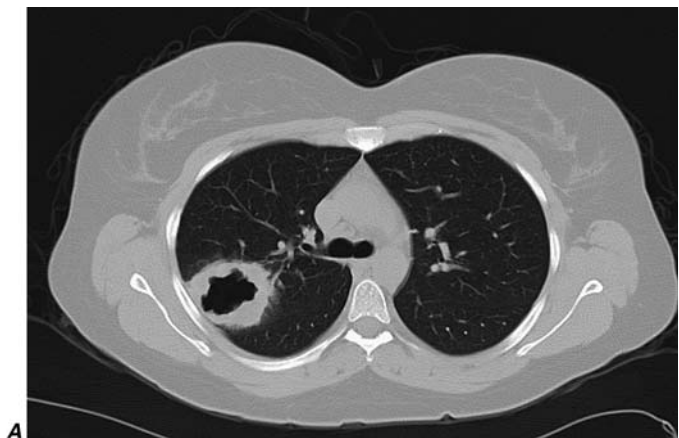


FIGURE e28-2 Computed tomography of the chest in two patients with Wegener's granulomatosis demonstrating (A) single and (B) mul-

iple cavitary lung lesions.

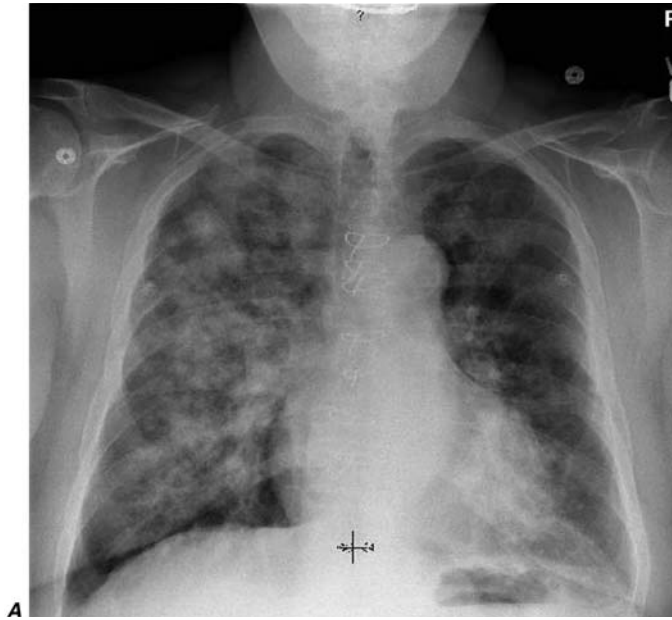


FIGURE e28-3 Bilateral ground-glass infiltrates due to alveolar hemorrhage from pulmonary capillaritis as seen in the same patient by (A) chest radiograph and (B) computed tomography.

This manifestation can occur in Wegener's granulomatosis or microscopic polyangiitis.

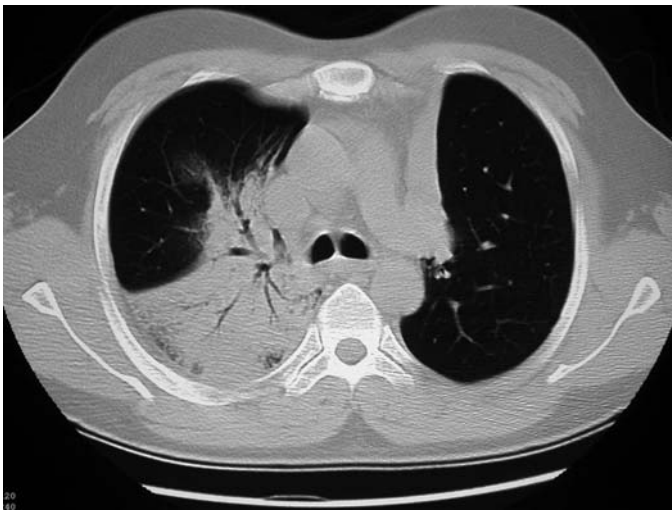


FIGURE e28-4 Computed tomography of the chest demonstrating a dense infiltrate with air bronchograms involving a segment of the right upper lobe due to bacterial pneumonia in an immunosuppressed patient with Wegener's granulomatosis. Collapse of the left upper lobe secondary to endobronchial stenosis from Wegener's granulomatosis also is seen on this image.

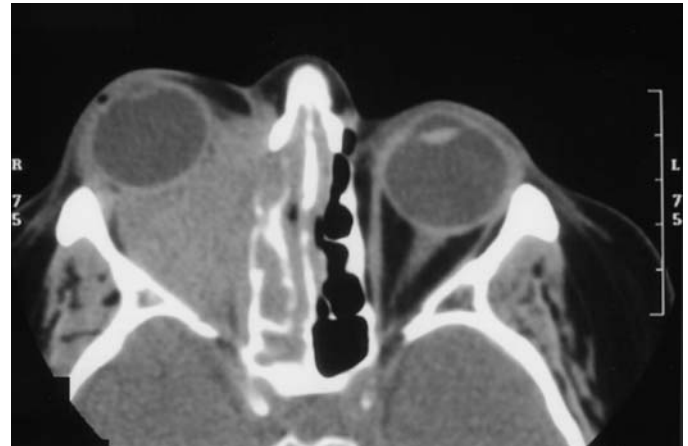


FIGURE e28-5 Computed tomography of the orbits in a patient with Wegener's granulomatosis who presented with right eye proptosis. The image demonstrates inflammatory tissue extending from the ethmoid sinus through the lamina papyracea and filling the orbital space.

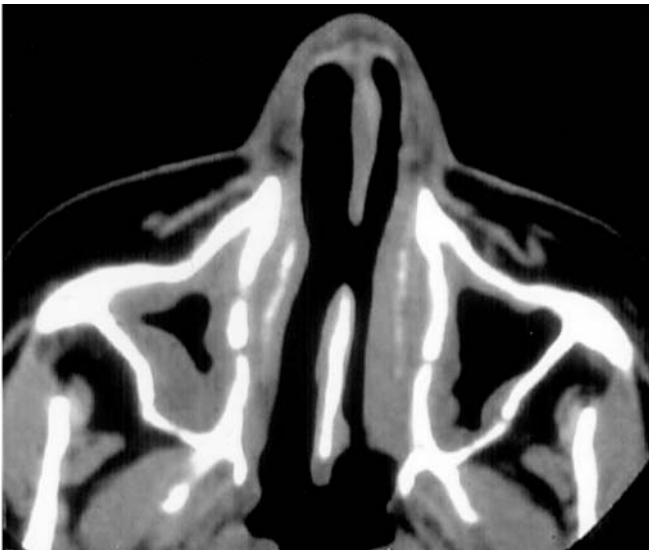
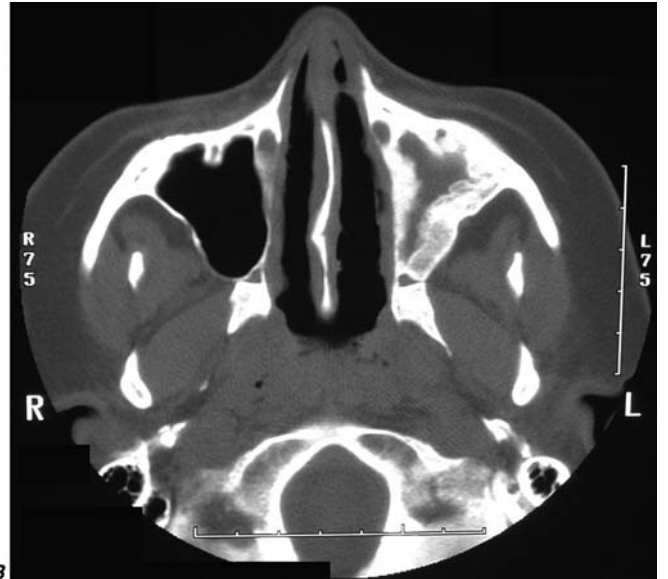


FIGURE e28-6 Computed tomography of the sinuses in two patients with Wegener's granulomatosis. (A) Mucosal thickening of the bilateral maxillary sinuses and a perforation of the nasal septum.



(B) Osteitis with obliteration of the left maxillary sinus in a patient with long-standing sinus disease.

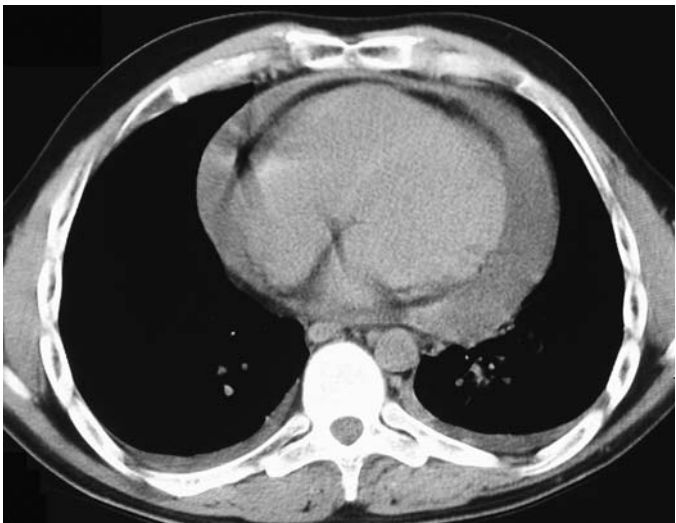


FIGURE e28-7 Computed tomography of the chest demonstrating a large pericardial effusion in a patient with Churg-Strauss syndrome. Cardiac involvement is an important cause of morbidity and mortality in Churg-Strauss syndrome and can include myocarditis, endocarditis, and pericarditis.

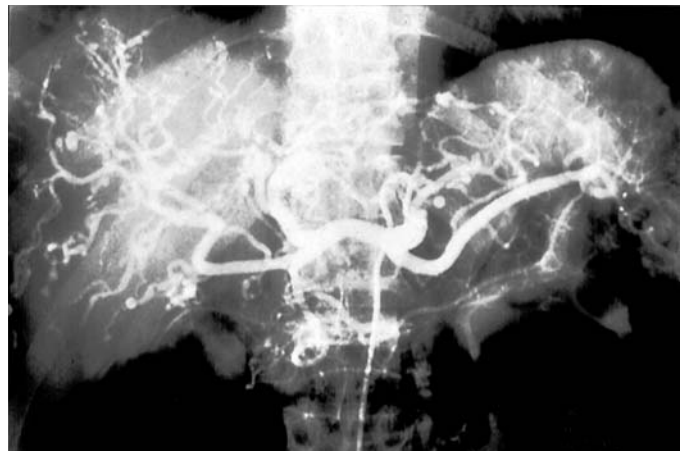


FIGURE e28-8 Arteriogram of a 40-year-old man with polyarteritis nodosa demonstrating microaneurysms in the hepatic circulation.



FIGURE e28-9 Cerebral arteriogram demonstrating beading along branches of the internal carotid artery in a patient with isolated central nervous system vasculitis.



FIGURE e28-11 Magnetic resonance imaging demonstrating extensive aneurysmal disease of the thoracic aorta in an 80-year-old female. The patient had been diagnosed with biopsy-proven giant cell arteritis 10 years prior to presenting with this aneurysm.

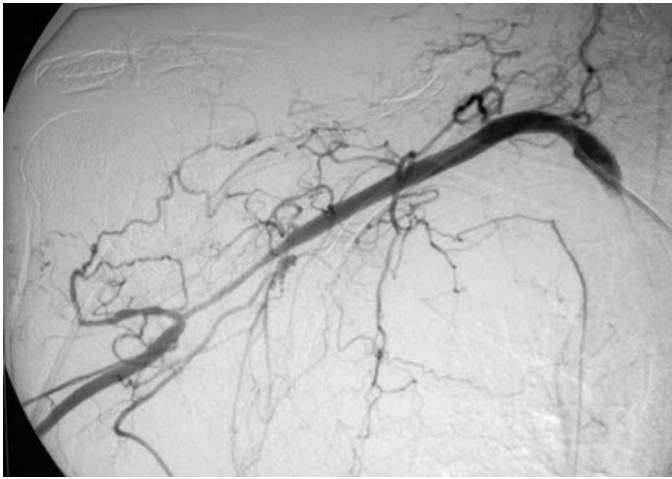


FIGURE e28-10 Upper-extremity arteriogram demonstrating a long stenotic lesion of the axillary artery in a 75-year-old female with giant cell arteritis.



FIGURE e28-12 Arteriogram of the aortic arch demonstrating complete occlusion of the left common carotid artery just after its origin from the aorta. This 20-year-old female presented with syncope and was subsequently diagnosed with Takayasu's arteritis.



FIGURE e28-13 Arteriogram demonstrating stenosis of the abdominal aorta in a 25-year-old female with Takayasu's arteritis.

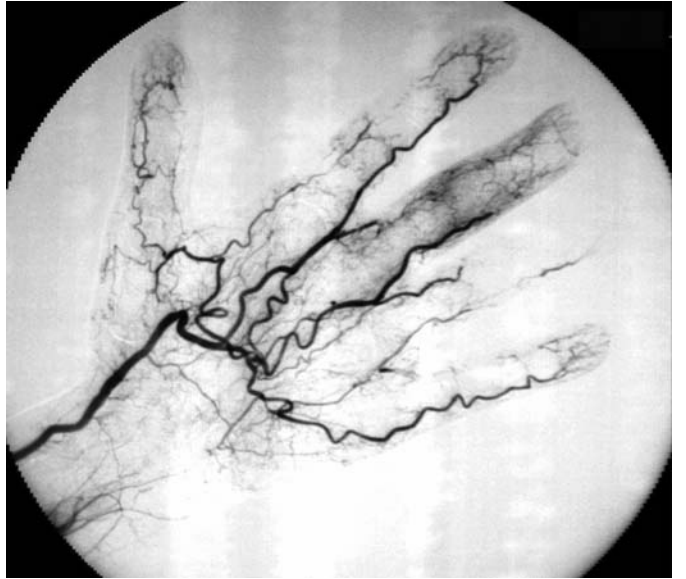


FIGURE e28-14 Arteriogram of the hand demonstrating arterial skip lesions and vessel cutoffs in a patient with cryoglobulinemia due to multiple myeloma.

